Translational Oncology 14 (2021) 101159

Contents lists available at ScienceDirect

Translational Oncology

journal homepage: www.elsevier.com/locate/tranon

Original Research

Targeting IFN-γ-inducible lysosomal thiol reductase overcomes chemoresistance in AML through regulating the ROS-mediated mitochondrial damage

Li-Ting Niu [a], Yu-Qing Wang [a,b], Catherine C.L. Wong [b,c,d,e], Shuai-Xin Gao [c], Xiao-Dong Mo [a], Xiao-Jun Huang [a,b,*]

[a] Peking University People's Hospital, Peking University Institute of Hematology, National Clinical Research Center for Hematologic Disease, Beijing Key Laboratory of Hematopoietic Stem Cell Transplantation, Beijing, 100044, China
[b] Peking-Tsinghua Center for Life Sciences, Peking University, Beijing 100871,
[c] Center for Precision Medicine Multi-Omics Research, Peking University Health Science Center, Peking University, Beijing 100191, China.
[d] School of Basic Medical Sciences, Peking University Health Science Center, Beijing 100191, China
[e] Peking University First Hospital, Beijing, 100034, China

ARTICLE INFO

Keywords:
AML
Chemoresistance
LSC
GILT
Oxidative stress

ABSTRACT

The persistence of leukemia stem cells (LSCs) is one of the leading causes of chemoresistance in acute myeloid leukemia (AML). To explore the factors important in LSC-mediated resistance, we use mass spectrometry to screen the factors related to LSC chemoresistance and defined IFN-γ-inducible lysosomal thiol reductase (GILT) as a candidate. We found that the GILT expression was upregulated in chemoresistant CD34+ AML cells. Loss of function studies demonstrated that silencing of GILT in AML cells sensitized them to Ara-C treatment both *in vitro* and *in vivo*. Further mechanistic findings revealed that the ROS-mediated mitochondrial damage plays a pivotal role in inducing apoptosis of GILT-inhibited AML cells after Ara-C treatment. The inactivation of PI3K/Akt/nuclear factor erythroid 2-related factor 2 (NRF2) pathway, causing reduced generation of antioxidants such as SOD2 and leading to a shifted ratio of GSH/GSSG to the oxidized form, contributed to the over-physiological oxidative status in the absence of GILT. The prognostic value of GILT was also validated in AML patients. Taken together, our work demonstrated that the inhibition of GILT increases AML chemo-sensitivity through elevating ROS level and induce oxidative mitochondrial damage-mediated apoptosis, and inhibition of the PI3K/Akt/NRF2 pathway enhances the intracellular oxidative state by disrupting redox homeostasis, providing a potentially effective way to overcome chemoresistance of AML.

Introduction

Acute myeloid leukemia (AML) is the most common type of hematological malignancy. [1] In addition to the conventional chemotherapy, the hematopoietic stem cell transplantation (HSCT) also improve clinical outcomes due to the immune-mediated graft-versus-leukemia (GVL) effect. [2,3] However, high rate of relapse still occurs partially attributive to the persistence of leukemia stem cells (LSCs), a group of cells that are generally in quiescence and that respond poorly to chemotherapeutic agents. [4] Generally, high frequency of LSC present in leukemic blasts at diagnosis is associated with an increased risk of relapse. [5] Therefore, there is a growing recognition that eradication of LSCs is critical for AML therapy with curative intent.

Oxidative stress, a condition where relatively excessive production of reactive oxygen species (ROS) is beyond cellular antioxidants, plays crucial roles in the chemotherapy-induced apoptosis of leukemic cells. [6] The dysregulation of ROS, small molecules that are overproduced upon stress response such as chemotherapeutic drugs, [7-10] has been described in many malignant diseases. [11] Large amounts of ROS can oxidize DNA, protein and lipids, inducing cell death. [12] In fact, cancer stem cells (CSCs) generally maintain a relatively low ROS level compared with the bulk cancer cells and the low ROS level in CSC was related to chemoresistance and disease recurrence. [13] Strikingly, previous studies found that ROS-low cells have higher engraftment

* Corresponding author at: Peking University People's Hospital, Peking University Institute of Hematology, No. 11 Xizhimen South Street, Xicheng District, Beijing, 100044, China.
E-mail address: huangxiaojun@bjmu.edu.cn (X.-J. Huang).

https://doi.org/10.1016/j.tranon.2021.101159
Received 13 June 2021; Accepted 14 June 2021
Available online 9 July 2021

potential and are LSC-enriched, indicating that regulation of intracellular ROS is critical for LSC to maintain proliferative capacities. [14-17] However, whether the low ROS level in LSC was responsible for therapeutic resistance and the underlying mechanism have not been fully investigated. Disruption of cellular redox hemostasis of LSC may provide a potential way to sensitize them to chemotherapeutic agents.

IFN-γ-inducible lysosomal thiol reductase (GILT) encoded by *IFI30* gene is known as an enzyme that catalyzes disulfide bond reduction. [18] The ablation of GILT in fibroblasts and T cells led to oxidative stress, as evidenced by increased production of ROS with decreased expression of antioxidants such as SOD2 and reduced glutathione (GSH). [19-21] In addition, it has been indicated that after treating relapsed/refractory AML patients with MEC (mitoxantrone, etoposide, and cytarabine), GILT showed significantly differential expression between responding and resistant patients. [22] However, whether GILT plays roles in the chemoresistance of LSC remains unclear. Although the surface markers of LSC are still controversial, leukemia stem cells have been found to be enriched in the CD34+ compartment [23-28] and CD34+ LSC are generally served as leukemic progenitors. [29]

In this study, we screened a factor GILT that was upregulated in LSC-enriched CD34+ chemoresistant AML cells through mass spectrometry. Our data confirmed that the knockdown of *GILT* by genetic silencing, producing a higher level of ROS and resulting in mitochondrial damage and apoptosis, enhanced the sensitivity of AML cells to Ara-C treatment both *in vitro* and *in vivo*. The PI3K/Akt/NRF2 pathway was remarkably inhibited in GILT-inhibited cells, which in turn, the antioxidant level was reduced, and this possibly contributes to this unbalanced redox state. Finally, we found that low GILT expression at diagnosis is associated with a better prognosis of AML.

Materials and methods

Mass spectrometry measurements

Add 500 μl cold RIPA Buffer (ThermoFisher Scientific, Cat#89901, USA) to the cells, keep on ice for 5 minutes, centrifuge samples at 14,000 × g for 15 minutes to pellet the cell debris. After the concentration of the supernatant was measured, the 50ug protein was precipitated. The next steps including sample preparation for data-independent acquisition (DIA) analysis, sample preparation for spectral library and high-PH reversed-phase fraction were conducted according to the method reported by our team previously. [30] Then, the EASY-nLC1200 liquid chromatography system (ThermoFisher Scientific, USA) was employed for Liquid chromatography. All samples were analyzed on Thermo QExactive HF-X (ThermoFisher Scientific, USA). As for the generation of spectral Library and DIA data Analysis, spectral libraries were generated with Spectronaut version 14.0 (Biognosys) using the default parameters. MS/MS spectra were matched against the human UNIPROT database (only reviewed entries) (human 20,421 entries, downloaded in July 2019). The subsequent procedure of statistical analysis was referring to previously reported method by our group. [30]

Cell lines, primary human AML cells and culture conditions

The human AML cell lines Kasumi-1, NB4, OCI-AML3, MOLM13, THP-1, U937 and MV411were purchased from the agent of American Type Culture Collection (ATCC) in China. All the cell lines have passed the STR authentication. Cell lines were cultured in RPMI 1640 medium (ThermoFisher Scientific, Cat#11875093, USA) containing 10% FBS (ThermoFisher Scientific, Cat#12483020, USA) and 1 × antibiotic–antimycotic (ThermoFisher Scientific, Cat#15240096, USA). Cells were grown at 37°C in a humidified atmosphere with 5% CO2.

The AML patients were diagnosed and treated at the Hematology Department of Peking University People's Hospital, Beijing, China. According to the Declaration of Helsinki, informed consent of all patients in the study was obtained. The study was approved by the local ethics review board (Reference number: 2020PHB010-01).

The inclusion criteria for diagnostic sample that must be met are the following: (i) Patients 16 to 80 years of age who had newly diagnosed but not therapy related AML in Peking University People's Hospital between September 2019 and September 2020; (ii) They had not previously received antineoplastic therapy beside hydroxyurea therapy that was allowed for 5 days before. (iii) They are not diagnosed with other major coexisting illness such as severe kidney and liver insufficiency. (iv) They have provided written informed consent. We also had an inclusion criteria particular for proteome analysis: (i) the patients who received the first induction chemotherapy "IA protocol" treatment in our hospital; (ii) In the diagnostic bone marrow sample, the percentage of CD34+ cells in nucleated cells was more than 20%; The criteria for CR after AML therapy is defined as: (i) <5% blasts morphologically in bone marrow; (ii) neutrophil count >1000/μL and platelet count >100,000/μL in the PB; (iii)without extramedullary AML.

Bone marrow mononuclear cells (BMMCs) were isolated by Ficoll density gradient centrifugation and cultured with IMDM (Thermo Fisher Scientific, Cat#12440053, USA) with 10% BIT 9500 (Stem Cell Technologies, Cat#099500, Canada). Cells were grown at 37°C in a humidified atmosphere with 5% CO2.

Drug compounds

Ara-C (cytarabine), Doxorubicin (DOX), N-acetylcysteine (NAC) and Tert-butylhydroquinone (tBHQ) were all purchased from Selleck Chemicals (Selleck, USA).

Lentiviral transduction

MOML13 and U937 cells were transfected with *GILT* shRNA lentiviral particles (Genechem, China) or blank control lentiviral particles (Genechem, China) using a GV493 system with GFP containing different shRNA sequences. The target sequences are as follows: shGILT#1: ccAGACACTATCATGGAGTGT shGILT#2: ccCTACGGAAACGCACAGGAA shNC: TTCTCCGAACGTGTCACGT

The AML cells were seeded the day before transduction with the density of 2 × 10^5/mL in the 6-well plates. On next day, the lentivirus and 8 ug/mL Polybrene (Sigma, TR-1003) were added (multiplicity of infection (MOI) is equal to 50) to cells. Cells were incubated in 37°C for 8 h, prior to the half removal of the upper-supernatant and refreshed with complete cell medium. When cells recovered to normal growth rate, discarding the supernatant and replaced with new medium. Cells were cultured for about two weeks and then isolated by GFP+ sorting.

Xenotransplantation assays

For the survival curve, forty-two male eight-week-old NOD.Cg-PrkdcscidIl2rgttm1Vst/Vst (NPG) mice (Beijing Vital Laboratory Animal Technology Company, China) were used in this study, of which thirty-two were randomly divided into four groups. For the analysis of leukemia burden, another ten mice were randomly divided into two groups for leukemic burden analysis. Then the mice were transplanted with 5 × 10^5/100μL of MOLM13-shGILT#2 or MOLM13-shNC cells via tail-vein injection after 100cGy irradiation on Day 1. The mice were monitored daily for assessment of leukemia. Ara-C (80mg/kg) or PBS were applied once daily on Day 7, Day 8 and Day 9 intraperitoneally, and mouse survival was monitored (n=8). Mice were euthanized on Day 23 for the leukemia burden as green fluorescent protein (GFP)/hCD45-positive cells by flow cytometry in the bone marrow (n=5) and the assessment of spleen size and the infiltration in liver, bone marrow and spleen (n=3). All animal experiments were evaluated and approved by the Animal Ethics Committee of Peking University People's Hospital (Reference number: 2020PHE038) and reporting adhered to the ARRIVE 2.0 guidelines [31]. All the animal experiments were performed in a sterile environment. Besides, the cages of mice were kept in a SPF-grade

laboratory animal room. The water, food and bedding were changed every other day.

Flow cytometry

Apoptosis assay

1×10^6 cells were resuspended with binding buffer (BD Biosciences, Cat#556454, USA) and stained with Annexin V-APC (BD Biosciences, Cat#550474, USA) for 15 min at 25°C in the dark for flow cytometry analysis.

Cellular and mitochondrial ROS staining

The Cellular Reactive Oxygen Species Detection Assay Kit (Abcam, Cat#ab186029, UK) and MitoSOX (Thermo Fisher Scientific, Cat#M36008, USA) were used to detect the cellular and mitochondrial ROS according to the manufacturer's instructions respectively. Briefly, cells were treated with or without Ara-C for 48h, and probed with CellROX for 20min or 5 μM MitoSOX for 15 min at 37°C and then washed by PBS+0.2% BSA before flow cytometry analysis.

NRF2 and P-Akt staining

Cells were suspended and incubated with fixation/permeabilization solution (BD Biosciences, Cat#554722, USA) for 30 min at room temperature, washed twice with BD Perm/Wash buffer (BD Biosciences, Cat#554723, USA) and stained with NRF2-APC (Abcam, Cat#ab223927, UK) or P-Akt-BV421 (BD Biosciences, Cat#562599, USA) for 30 min for flow cytometry analysis.

TMRE staining

TMRE Mitochondrial Membrane Potential Assay Kit (Abcam, Cat#ab113852, UK) was used at 100 nM for 20 minutes at 37°C in growth media for assessing mitochondrial membrane potential (MMP), then washed with PBS+0.2% BSA. FCCP (20 mM) treatment was used for control of TMRE-specific staining.

MitoTracker staining

Cells were stained with 200nM MitoTracker Deep Red (Thermo Fisher Scientific, Cat#M22426, USA) at room temperature for 15 min and then analyzed by flow cytometry to assess the mitochondrial mass.

Cell viability assay

Cell viability was determined by CCK-8 assay (Bimake, Cat#B34034, USA). The cells were seeded in a density of 2×10^4 cells/100μL in a 96-well plate and incubated at 37°C for 48h. 10μL CCK-8 was added to each well of the 96-well plate, followed by further incubation for 1 h. The absorbance was measured at 450nm. The half-maximal inhibitory concentration (IC50) was calculated using GraphPad Prism software.

GSH/GSSG assay and NADPH/NADH assay

Ara-C-treated cells were collected and washed twice with PBS. According to the manufacturer's instructions, the GSH/GSSG ratio and was evaluated using a GSH/GSSG assay kit (Beyotime Institute of Biotechnology, Cat#S0053, China) and the NADPH/NADH ratio was evaluated using NADPH/NADH assay kit (Beyotime Institute of Biotechnology, Cat#S0179, China)

Western blot

The procedures of preparing and analyzing total cell lysates were as described previously. [32] Antibodies were obtained from Santa Cruz Biotechnology (Santa Cruz, USA) and Cell Signaling Technology (CST, USA). Antibodies: GILT (Santa Cruz: Cat#SC-393507), Cleaved-Caspase3 (Cell Signaling Technology: Cat#9664, USA), Cleaved-PARP (Cell Signaling Technology: Cat#5625, USA), SOD2 (Cell Signaling Technology: Cat#13141, USA), Actin (Cell Signaling Technology: Cat#3700, USA), AKT (Proteintech, Cat#60203, China), P-AKT (Proteintech, Cat#66444, China), PI3K (Proteintech, Cat#60225, China), P-PI3K (Cell Signaling Technology: Cat#4228, USA)

RNA preparation and Q-PCR

Total cellular RNA was extracted using the RNeasy Mini Kit (QIAGEN, Cat#74104, Germany) following the manufacturer's protocol. The cDNA was synthesized through reverse transcription of 500ng of RNA using PrimeScript RT reagent Kit with gDNA Eraser (Takara, Cat#RR047a, Japan).

Only samples of purified RNA with high-quality integrity were used for cDNA synthesis and qPCR. RNA integrity was evaluated by blot analysis with clear 28S and 18S rRNA bands at a ratio of ~2:1, and RNA purification was measured by an A260/280 absorbance ratio of 1.8–2.0. The quantitative real time RT-PCR was conducted using the 7500 real PCR System (Applied Biosystems) and complied with the Minimum Information for Publication of Quantitative Real-Time PCR Experiments (MIQE) guidelines [33]. The RT-PCR amplifications were set up in a total volume of 20 μL consisting of 1 μL cDNA, 2 μL primer mix, 7 μL of water, and 10 μL of SYBR Master Mix (Thermo Fisher Scientific, Cat#A25742, USA). Samples were assayed in triplicate in 96 well plates (Applied Biosystems) and average Ct values were calculated for analyses. For each measurement the threshold of amplification curve was set at 0.1.

Relative gene expression was assessed using the $2^{-\Delta\Delta Ct}$ method, and average gene transcript levels in control group were used as calibrator for comparison. The gene transcript levels of patient samples were determined by absolute quantitation. For each qPCR, a standard curve was plotted using a series of known cDNA dilutions as the template to calculate initial concentration of the targets in each sample. The level of each target was calculated from standard curve using the Ct values.

Sequences of the primer pairs used were as follows: human IFI30: (NCBI accession number: 10437)

Forward: GAAGTCCAATGCACCGCTTG

Reverse: TGTTCCTGTGCGTTTCCGTA human GAPDH: (NCBI accession number: 2597)

Forward: CCCATGTTCGTCATGGGTGT

Reverse: GATGGCATGGACTGTGGTCA

Immunohistochemistry

Tissue samples were fixed with 4% paraformaldehyde at room temperature and incubated with PBS containing 10% goat serum, 0.3 M glycine, 1% BSA and 0.1% triton for 1hour at room temperature to permeabilize the cells and block non-specific protein-protein interactions. And with 3% H_2O_2 at room temperature for 5min. Samples were incubated with anti-CD45 antibody (Biolegend, Cat#304037, USA) at 4C overnight and then incubated with horseradish peroxidase-conjugated anti-mouse secondary antibody, and the antibody binding was visualized using DAB. Finally, images were taken by light microscope (Eclipse 80i, Japan). Image analysis was conducted with Image-Pro Plus 6.0 software to determine the mean integrated optical density (IOD) value (arbitrary units).

Immunofluorescence staining

Cells were fixed with 4% paraformaldehyde and cytospun onto slides, then permeabilized with Triton 0.1% for 30min and incubated with primary antibodies anti-NRF2 (Abcam, Cat#62352, UK) followed by indicated secondary antibodies. Then DAPI was used to label cell nuclei. Cells were observed using a fluorescence microscope at the same exposure.

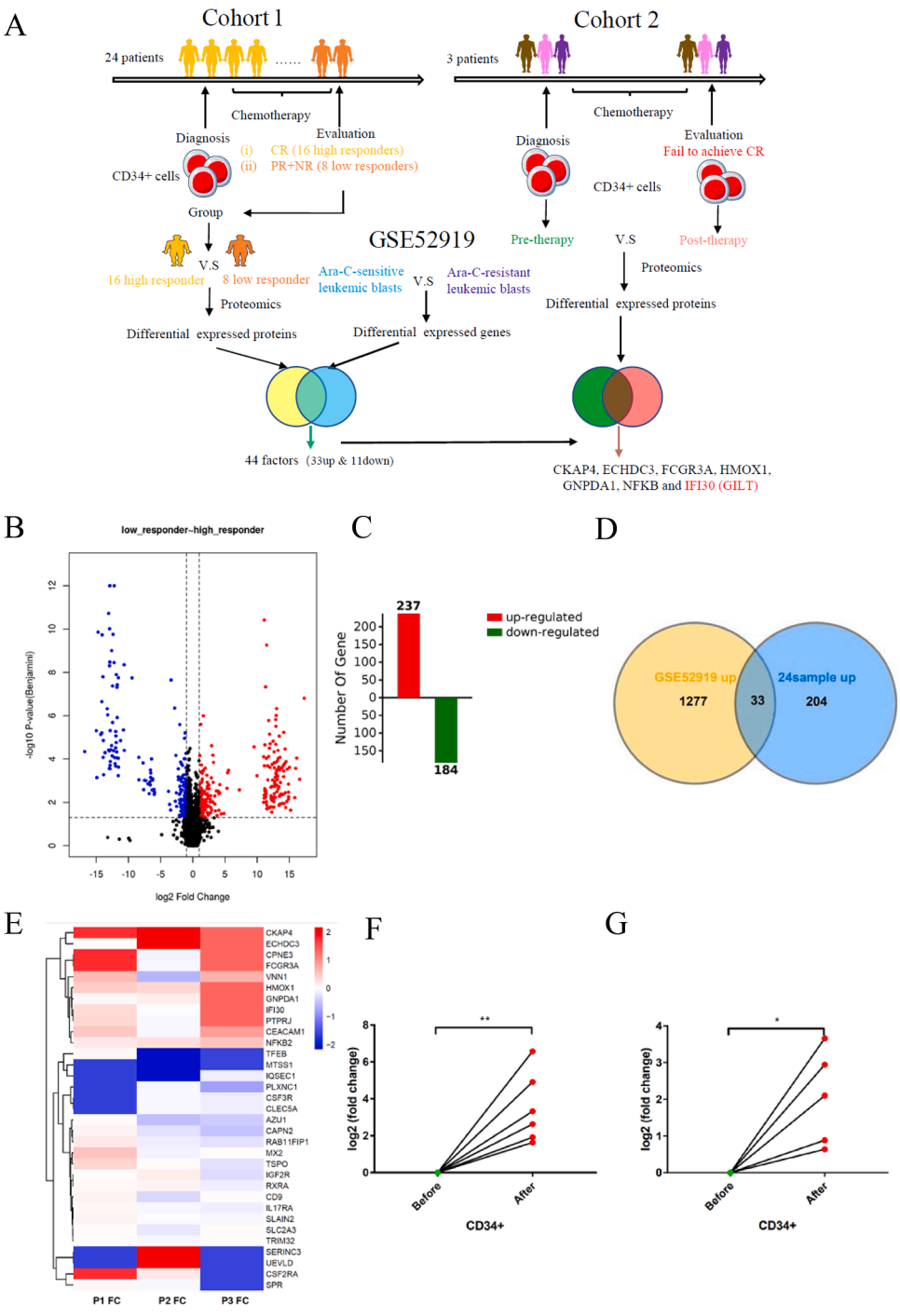

Fig 1. GILT is upregulated in chemoresistant CD34+ AML cells

(A) Schematic presentation of our experimental design. Protein expression levels of LSC-enriched CD34+ cells were compared between 16 high responders and 8 low responders (cohort 1). The data-independent acquisition (DIA) technique was applied for quantitative proteomics, which was performed by a trapped ion mobility spectrometry coupled to TOF mass spectrometry (TIMS-TOF MS) with the parallel accumulation-serial fragmentation (PASEF) technique. GSE52919 showed the differential expressions between Ara-C-resistant and Ara-C-sensitive leukemic blasts. 44 factors including 33 upregulated factors and 11 downregulated factors were screened out by analyzing above two data sets. The quantitative proteomics was also performed to compare the protein alterations of therapy-free CD34+ cells and post-chemotherapeutic CD34+ cells, with samples from three individuals who failed to achieve CR taken at the time before and after the first induction chemotherapy, respectively (cohort 2). Seven mediators were validated to show an overexpressed pattern in chemotherapy-challenged survival AML cells.

(B) Volcano plot of selected proteins in comparison between 16 high responders versus 8 low responders. Fold change >2, fold change <0.5 and p value (t test) <0.05 were used to filter differential expression proteins. The y-axis represents the probability that the protein was differentially abundant. The red points and blue points sections represent proteins that were significantly increased or decreased in low responders, respectively.

(C) Diagram showed upregulated proteins (red) and downregulated proteins (green) in the low responders compared with the high responder group.

(D) Venn diagram showed significantly upregulated proteins in chemo-insensitive cells were selected with a fold change >2 and p-value <0.05 among cohort 1 (blue) and GSE52919 (yellow). 33 factors were overexpressed in both low responders of cohort 1 and Ara-C-resistant leukemia blasts of the expression profile GSE52919 sets.

(E). Heatmap depicting the relative fold change of 33 altered factors selected in D. Color bar represents the relative intensity of identified proteins from −2 to 2.

(F). Q-PCR analysis revealing the fold change of GILT mRNA level in six paired pre-therapy and post-therapy CD34+ BMMC samples.

(G). Q-PCR analysis of *GILT* mRNA level in sorted CD34+ BMMCs that were obtained from newly diagnosed AML patients (n=5) treated with or without Ara-C (2000nM) for 48 hours. Data represent the mean ± SEM. Student's t-test was used to determine statistical significance: *p<0.05. CR, complete remission; BMMC, bone marrow mononuclear cells.

Statistical analysis

GraphPad Prism 7.0 were mainly used for statistical analysis. Kaplan-Meier survival analysis was used to evaluate the prognostic value. Student t tests are presented as the mean ± SEM to compare the differences between two groups and values with $p < 0.05$ are considered significant. Gaussian distribution between variables were examined for appropriate statistical analysis.

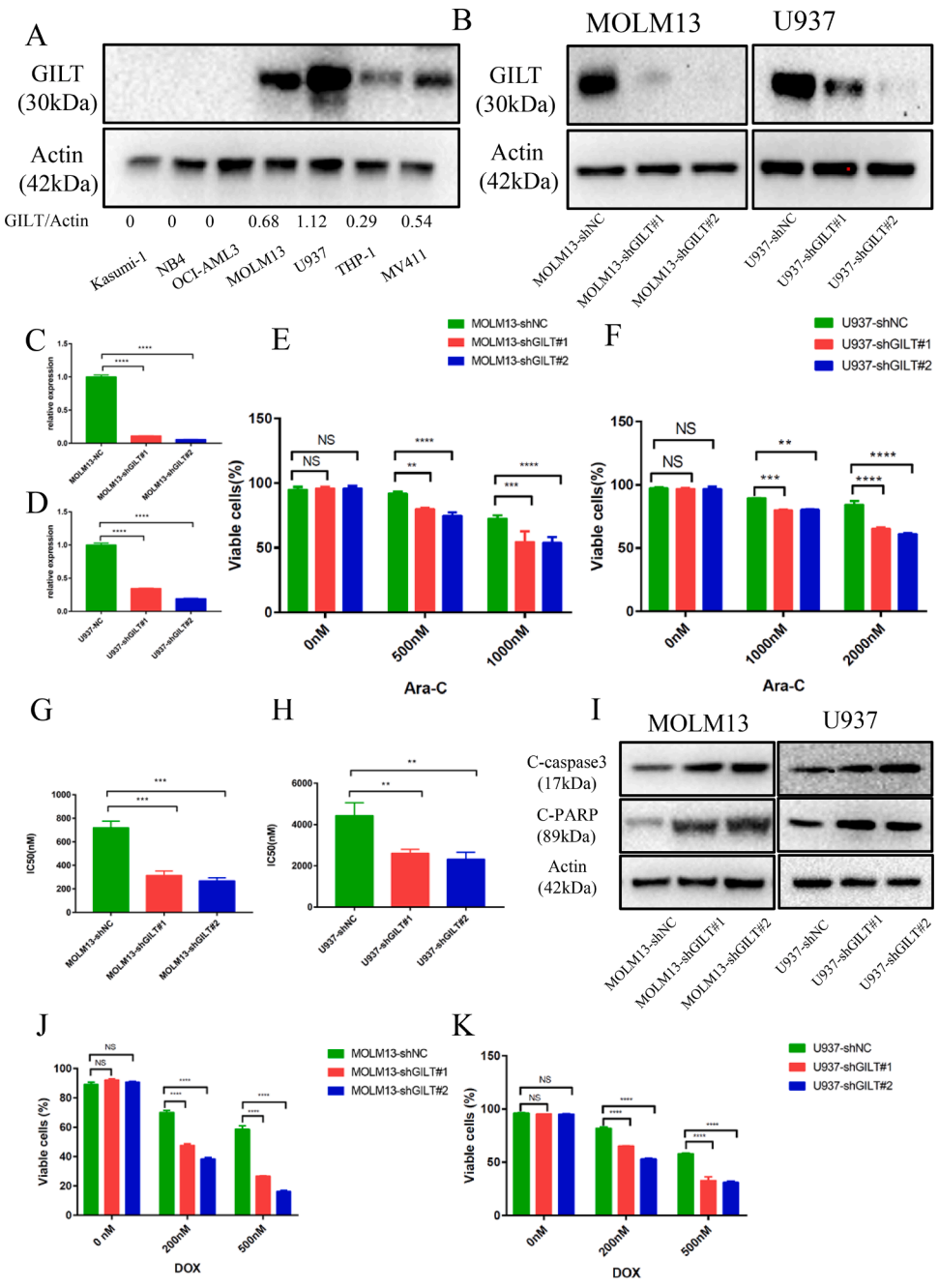

Fig 2. GILT suppression enhances chemosensitivity of AML cells

(A) Western Blot analysis of GILT expression in human AML cell lines.

(B-D) Western blot and q-PCR analysis showing suppression of GILT in two AML cell lines at both protein (B) and mRNA level (C, D). GILT knockdown was performed by introducing either scramble (NC group) or two different *GILT* shRNAs into MOLM13 and U937 cell lines.

(E. F) The proportion of viable cells after a 48-hour treatment with different doses of Ara-C in modified MOLM13 cells (E) and U937 cells (F).

(G.H) IC50 values of modified MOLM13 cells (G) and U937 cells (H) after exposure to Ara-C for 48 hours.

(I) Western blot analysis was used to detect the cleavage of Caspase 3 and PARP in modified MOLM13 cells (left) and U937 cells (right) after exposure to Ara-C for 48 hours.

(J.K) The proportion of viable cells after a 48-hour treatment with different doses of daunorubicin (DOX) in modified MOLM13 cells (J) and U937 cells (K).

Data represent the mean ± SEM. Two-way ANOVA and Student's t-test was used to determine statistical significance: $^{**}p<0.01$, $^{***}p<0.001$, $^{****}p<0.0001$. GILT, IFN-γ-inducible lysosomal thiol reductase; AML, acute myeloid leukemia; IC50, 50% inhibitory concentration.

Results

GILT is upregulated in chemoresistant CD34+ AML cells

Accumulating evidence shows that LSCs are resistant to chemotherapy and are responsible for leukemia relapse. [34-36] In order to investigate the critical factors attributed to LSC-related chemoresistance, we collected the bone marrow mononuclear cells (BMMCs) from 24 AML patients (Table S1) at diagnosis including 16 high responders and 8 low responders (cohort 1). Patients grouped in high responders showed CR after the first intensive chemotherapy, with low responders defined as failing to achieve CR. Then the LSC-enriched CD34+ progenitors were isolated from BMMCs, followed by comparison of the protein levels in CD34+ cells between high and low responders using proteome analysis (Fig 1A). All the raw data were first processed using a double boundary Bayes imputation method (Fig S1A-S1B) and were standardized for further analysis (Fig S2A-S2D). Our data showed a clear stratification among different cohorts according to the principal component analysis (Fig S3A-S3B). We identified 6889 proteins in these samples, among which 237 proteins were significantly upregulated and 184 proteins were downregulated, in low responders compared with high responders (Fig 1B-1C). Next, we explored the publicly available database GSE52919, a mRNA expression profile comparing transcript levels between Ara-C-resistant and Ara-C-sensitive leukemia blasts, to further find mediators that are associated with chemoresistance. [37] We found that among 237 upregulated proteins in low responders, 33 proteins were upregulated in Ara-C resistant leukemic blasts comparing with Ara-C resistant group (Fig 1D), while 11 among 184 downregulated proteins were found that are overlapped with factors expressed at higher level in Ara-C resistant group (Fig S4A). Considering that chemotherapy reshapes the LSCs that alter their metabolic status to survive, we designed cohort 2 (Fig. 1A), with 3

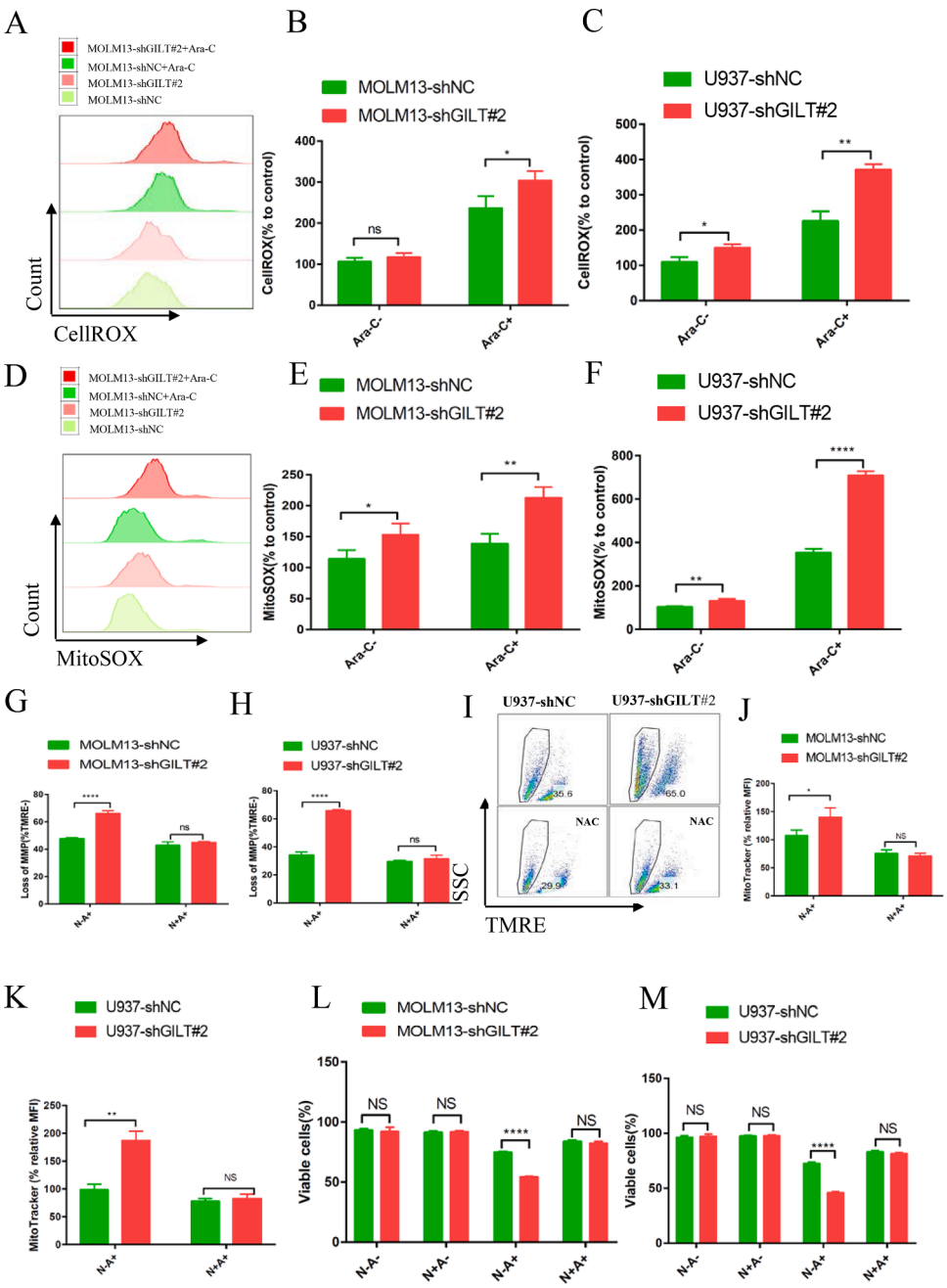

Fig 3. GILT knockdown strengthened Ara-C-mediated apoptosis by triggering ROS-mediated mitochondrial damage

Modified MOLM13 or U937 cells were treated with or without 1 μM Ara-C (MOLM13) or 2 μM Ara-C (U937) for 48 hours.

(A-C) CellROX staining was used to detect the cellular ROS level before flow cytometry analysis and shown as histogram (A), and the percentage of mean fluorescence intensity (MFI) relative to untreated MOLM13-shNC cells or U937-shNC cells was calculated (B, C).

(D-F) MitoSOX staining was used to evaluate the mitochondrial ROS level before flow cytometry, the results were depicted as histogram (D), and the percentage of MFI relative to untreated MOLM13-shNC cells or U937-shNC cells was illustrated (E, F).

(G-M) Modified MOLM13 or U937 cells were pretreated with or without 5 mM N-acetyl cystine (NAC) for 2 hours prior to exposure to 1 uM Ara-C (MOLM13) or 2 uM Ara-C (U937) for 48 hours. Loss of mitochondrial membrane potential (MMP) were determined by TMRE fluorescent probes before flow cytometry analysis in modified MOLM13 cells (G) and U937 cells (H, I). Mitochondrial mass was determined by MitoTracker Deep Red staining before flow cytometry analysis in modified MOLM13 cells (J) and U937 cells (K). The percentage of live cells was measured by flow cytometry in modified MOLM13 cells (L) and U937 cells (M). Data represent the mean ± SEM. Student's t-test was used to determine statistical significance: *p<0.05. **p<0.01, ****p<0.0001, ns, no significance. ROS, reactive oxygen species. MFI, mean fluorescence intensity; NAC, N-acetyl cystine; MMP, mitochondrial membrane potential.

patients (Table S1) providing paired samples taken at diagnosis and at the time of confirmation that fails to achieve CR. Only 3 samples in cohort 1 met the requirement that more than 20% blasts and at least 20% CD34+ cells present in the BM samples were analyzed in cohort 2. The protein alterations of LSC-enriched CD34+ cells before (therapy-naïve) and after (chemo-reshaped and more resistant) chemotherapy were analyzed using the same way (Fig S1C-S1D, FigS3C-S3D) to identify the changes in LSCs in response to chemotherapy. The differential expressions of above-mentioned 33 upregulated and 11 downregulated factors were further validated in cohort 2 by showing a heatmap (Fig 1D-1E, Fig S4A-4B). No factor among 11 downregulated proteins was found to show a consistent alteration in cohort 2 (Fig S4B). Seven among the 33 upregulated factors were screened that were consistently increased in CD34+ progenitors after chemotherapy, including CKAP4, ECHDC3, FCGR3A, HMOX1, GNPDA1, NFKB and IFI30 (Fig 1E). The mRNA levels of these seven upregulated genes were further validated in six paired samples (Fig 1F and Fig S4C). We next focused on the role of *IFI30*-encoded GILT in chemoresistance of AML since the association of GILT and AML chemoresistance has not yet been deeply studied. To further confirm that GILT expression is associated with Ara-C resistance, primary CD34+ cells were cultured with and without Ara-C *in vitro*. Consistent with our previous data, GILT was upregulated in response to Ara-C treatment (Fig 1G). Similar results were also seen in AML cell lines such as MOLM13 and U937 cells both in mRNA and protein levels (Fig S5A-S5D). Taken together, these results strongly revealed that chemoresistant AML CD34+ progenitor cells elevated GILT expression, indicating that GILT may be a key factor of LSC to attenuate chemo-cytotoxicity.

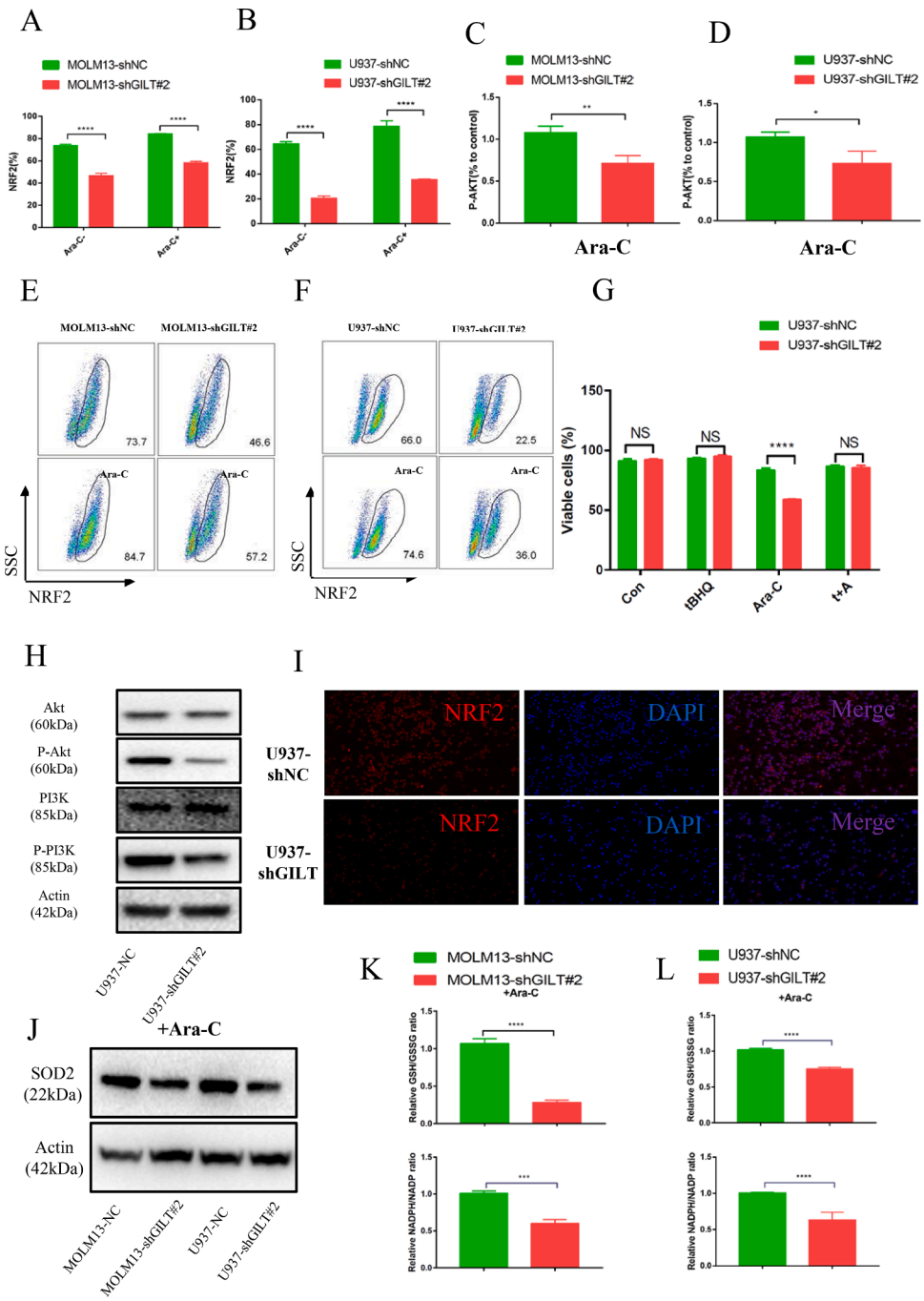

Fig 4. GLT inhibition induces oxidative stress involved inhibition of PI3K/Akt/NRF2 pathway.
Modified MOLM13 or U937 cells were treated with or without 1 μM Ara-C (MOLM13) or 2 μM Ara-C (U937) for 48 hours.
(A-B, E-F) Flow cytometric analysis of the percentage of NRF2-positive cells in modified MOLM13 cells (A, E) and modified U937 cells (B, F).
(C-D) Flow cytometric analysis of the MFI of P-AKT (relative to control) in modified MOLM13 cells (C) and modified U937 cells (D).
(G) After exposure to tBHQ (50 μM) and/or Ara-C (2000nM) for 48h, the proportion of viable cells were detected using flow cytometry in modified U937 cells.
(H) Western blot analysis of AKT, phosphorylated AKT (p-AKT), PI3K and phosphorylated PI3K (p-PI3K) expression in modified U937 cells.
(I) Immunofluorescence staining of NRF2 (red) in U937-NC cells and U937-shGILT cells treated with Ara-C for 48h. DAPI was used as a nuclear counterstain.
(J) Western blot depicted the SOD2 levels in two modified AML cell lines as indicated.
(K-L) The ratio of GSH/GSSG (upper panel) and NADPH/NADP (lower panel) was measured by the corresponding kits, and reduced glutathione/oxidized glutathione (GSH/GSSG) ratios and NADPH/NADP ratios were analyzed in two modified AML cell lines.
Data represent the mean ± SEM. Student's t-test was used to determine statistical significance: *p<0.05. **p<0.01, ****p<0.0001, ns, no significance. AML, acute myeloid leukemia; NRF2, nuclear factor erythroid 2-related factor 2; tBHQ, Tert-butylhydroquinone.

GILT suppression enhances the sensitivity of AML cells in response to chemotherapy in vitro

To further investigated the function of GILT in chemoresistance, we examined the IC50 in response to Ara-C and analyzed the protein levels of GILT across seven AML cell lines. The results showed that the highest expression of GILT was detected in MOLM13 and U937 cell lines (Fig 2A), and the value of IC50 positively correlated with the GILT level in cell line (Fig S6A-6B). Consequently, we used lentivirus-transfected shRNAs to silence the *GILT* expression in MOLM13 and U937. The two shRNAs efficiently decreased the GILT level (Fig 2B-2D). Different doses of Ara-C were added to *GILT*-deficient AML cells and their negative control (NC) counterparts, and apoptosis and cell growth assays were performed. The percentage of viable cells were significantly lower in cells with GILT deletion than control group, indicating that GILT knocking-down enhanced the cellular apoptosis induced by Ara-C treatment (Fig 2E-2F). Furthermore, knocking down of GILT led to a significant reduction of 50% inhibitory concentration (IC50) comparing with the NC group in both cell lines (Fig 2G-2H), implying that deletion of *GILT* sensitized AML cells to Ara-C. Concomitant elevation of cleaved caspase-3 and cleaved PARP, mediators that are activated during apoptosis, were also detected in GILT-silencing cells by western blot, which could further confirm our results (Fig 2I). In addition, we also explored whether the deletion of GILT could enhance the sensitivity to daunorubicin (DOX), another first line-used chemotherapeutic agent treating AML. Although there is no significant correlation between the DOX IC50 and GILT level in AML cell lines (Fig S6C-6D), the cell apoptosis analysis showed that the GILT deletion could also improve daunorubicin sensitivity (Fig 2J-2K), confirming the role of GILT in chemoresistance. Taken together, all these results indicate that GILT

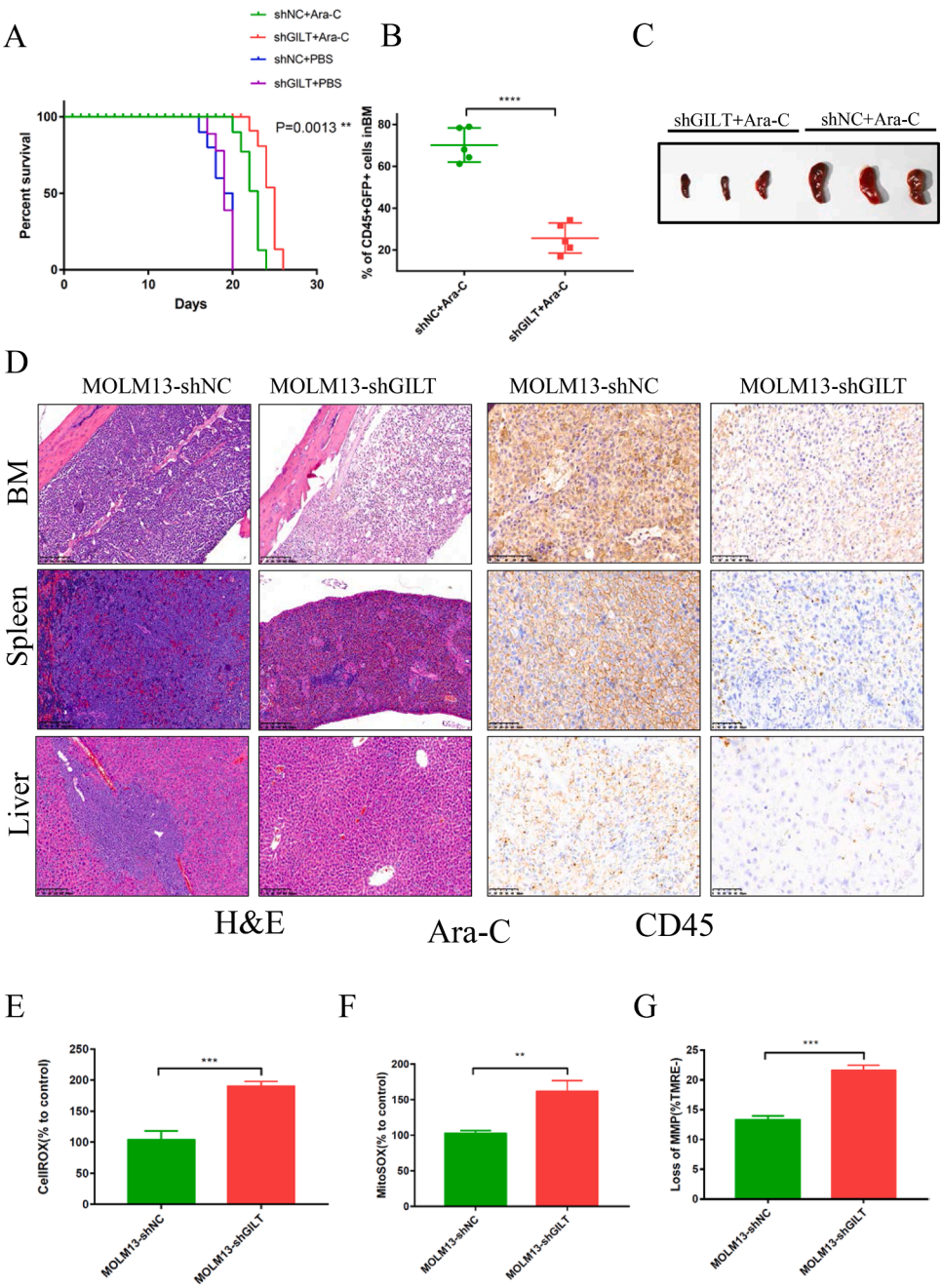

Fig 5. Silencing of GILT improves overall survival in a systemic human AML model
(A-D). NOD.Cg-Prkdcscidil2rgttm1Vst/Vst (NPG) mice were injected with MOLM13-shNC or MOLM13-shGILT#2 cells (5×10^5 cells) via tail vein. Ara-C (80 mg/kg) or PBS were used on Day 7, Day 8 and Day 9 by intraperitoneal injection. Kaplan-Meier plots for overall survival is shown in (A) (n=8). At Day 23 (Day 16 post-Ara-C therapy), the mice were sacrificed, and the tumor burden was measured by detection of double-positive (GFP/human CD45) cells in BM (n=5) (B). and the spleen size (C) and the tumor infiltration in BM, spleen and liver (D) of three mice from the Ara-C treated group were also assessed after euthanasia. Original magnification×10 for HE staining (left) and original magnification×20 for CD45 staining (right) for panel D.
(E-G) At Day 23 (Day 16 post-Ara-C therapy), after the mice were sacrificed, CellROX staining and MitoSOX staining were used to evaluate the cellular ROS level (E) and mitochondrial ROS level (F), loss of MMP was determined by TMRE fluorescent probes respectively in the leukemia blasts ($CD45^+GFP^+$) extracted from the mouse bone marrow in shGILT and NC group (n=3). The MFI was calculated in each of these cells. Data represent the mean ± SEM. Student's t-test was used to determine statistical significance: **p<0.01, ****p<0.0001, ns, no significance.

knocking-down forces the AML cells more sensitive to chemotherapy.

GILT knockdown strengthened Ara-C-induced apoptosis by triggering ROS-mediated mitochondrial damage

Previous studies have shown that GILT ablation in fibroblasts and T cells led to increased production of cellular ROS. [19-21] ROS is well known to play a crucial role in the regulation and induction of apoptosis in tumor cells. and modulating ROS levels render leukemia cells more susceptible to chemotherapy due to the distinct metabolic signatures of AML LSCs and blast cells compared to their normal counterparts. [15, 38-41] To ask whether inhibition of GILT in AML cells could elevate the ROS levels in the aim of sensitizing them to Ara-C treatment, the cellular ROS level were measured by CellROX staining prior to flow cytometry analysis. The results demonstrated that two AML cell lines with GILT knockdown increased cellular ROS level upon Ara-C treatment (Fig 3A-3C). The cellular ROS levels showed no significantly alteration in the MOLM13, with a slight elevation in the U937 cell line without addition of Ara-C (Fig 3A-3C). Moreover, as mitochondria are the main source of ROS generation, we also used the MitoSOX staining probe to analyze the mitochondrial ROS levels in the two AML cell lines. The two AML cell lines with *GILT* knocking down showed obvious increased mitochondrial ROS levels relative to the NC group both before and after Ara-C treatment (Fig 3D-3F), indicating that the elevation of cellular ROS level is perhaps mainly derived from mitochondria. Next, considering that mitochondria are also the primary targets of ROS damage, tetramethyl rhodamine ethyl ester (TMRE) was added to judge the mitochondrial membrane potential (MMP) and the MitoTracker probe was used to detect the mitochondrial mass upon Ara-C stimulation. Our data showed that compared with the NC group, loss of MMP and mitochondrial mass was more apparent in *GILT*-deleted cells with Ara-C treatment (Fig 3G-3I, Fig 3J-3K). Then we pretreated the AML cells with the N-acetyl

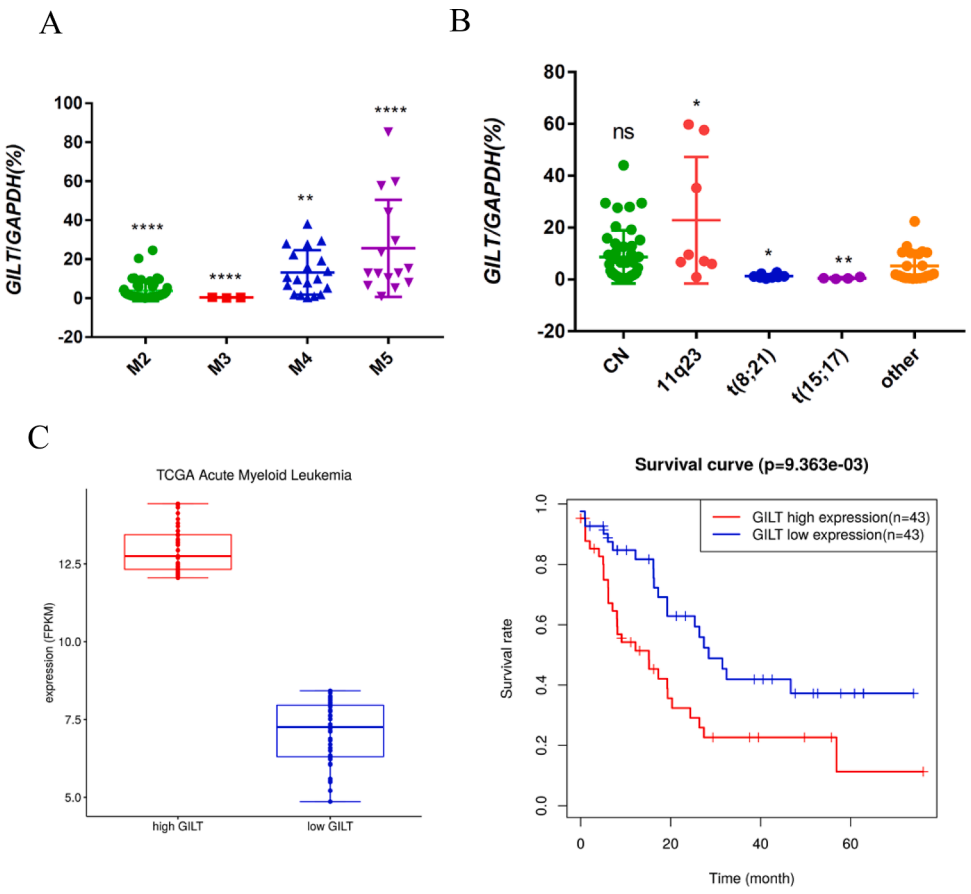

Fig 6. GILT is a potential prognostic marker of AML
(A-B) Q-PCR analysis of *GILT* mRNA expression levels across FAB-classified AML subtypes **(A)** and cytogenetic groups **(B)**. Shown P values represent significant differences between the indicated group and all other groups.
(C) Kaplan-Meier curves were used to assess the correlation between GILT expression and overall survival based on TCGA datasets.
Data represent the mean ± SEM. Student's t-test was used to determine statistical significance: *p<0.05. **p<0.01, ****p<0.0001, ns, no significance.

cysteine (NAC), which has been recognized as an ROS scavenger, prior to Ara-C treatment. NAC prevented the Ara-C induced loss of MMP, indicating that *GILT* down-expression could cause ROS-mediated mitochondrial damage, and this could be rescued by ROS inhibitor (Fig 3G-3I). We next investigated whether loss of MMP caused by excessive ROS generation could further induce the cell apoptosis. In line with the mitochondrial performance, GILT deficiency led to increased apoptosis in the context of Ara-C, and NAC pretreatment reversed the enhanced apoptosis induced by GILT suppression, illustrating that NAC inhibited the ROS-mediated pro-apoptotic effects by Ara-C (Fig 3L-3M). It is worth to point out that NAC alone was unable to influence apoptosis of AML cells as there was no significantly different apoptotic rate between the two groups with and without NAC pretreatment (Fig 3L-3M). Taken together, in the face of Ara-C, AML cells devoid of GILT over-produce ROS, and excessive ROS damage mitochondrial membrane potential, which in turn, promotes cell death.

GILT inhibition induces oxidative stress involved inhibition of PI3K/Akt/NRF2 pathway

Normal cells rewire the transcriptional networks to precisely regulate the production and metabolism of ROS, and pathways involved in these two processes act in unison to maintain the redox homeostasis. [42] The level of NRF2 is considered as a major mediator of ROS elimination by regulating the expressions of several antioxidants. [43] In this context, we expected to find that NRF2 is activated to neutralize over-produced ROS, in the aim of relieving cellular oxidative stress. Surprisingly, our results showed a decreased level of NRF2 in the GILT ablation group compared with the NC group with and without Ara-C treatment, reflecting the impaired antioxidant capacity after GILT ablation (Fig 4A-4B, 4E-4F and 4I). What's more, we treated NC and GILT-knockdown cells with Ara-C and NRF2 activator Tert-butylhydroquinone (tBHQ) [44], finding that activation of NRF2 could partially rescue the GILT mediated AML chemoresistance (Fig 4G). In addition, the PI3K/Akt signaling pathway has been reported to be essential for NRF2 transcriptional activation [45] Therefore, we next examined the activation of PI3K/Akt pathway using anti-phosphorylated Akt antibodies that recognize activated Akt by flow cytometry. Consistent with our hypothesis, the reduction of P-Akt has been observed in GILT inhibition group relative to the NC group in two AML cell lines after Ara-C treatment (Fig 4C-4D). Additionally, western blot results illustrating the level of Akt, phosphorylated AKT, PI3K and phosphorylated PI3K also confirmed the inhibition of this pathway (Fig 4H). SOD2, an antioxidant typically downstream of NRF2, [43] decreased in the absence of GILT, indicating an unbalance redox state (Fig 4J). We therefore analyzed the cellular oxidoreductive state of GILT-deleted cells which exhibited a decreased ratio in GSH/GSSG and NADPH/NADH (Fig. 4K-4L). Collectively, these results illustrate that GILT deletion induces an unbalanced redox state in AML cells upon Ara-C treatment, at least partly through the suppression of PI3K/Akt/NRF2 pathway.

GILT inhibition improves overall survival in a systemic human AML model

To test whether GILT inhibition in AML cells could also enhance the chemosensitivity *in vivo*, we established a human AML mouse model: NOD.Cg-PrkdcscidIl2rgttm1Vst/Vst (NPG) mice [46] were injected at the tail vein with MOLM13 cells that carry scramble shRNA or shGILT at Day 1. A dose of 80 mg/kg Ara-C were injected intraperitoneally to mice at the time of Day 7 after AML cells penetration for 3 consecutive days, and injection of PBS was served as an untreated control. Our Kaplan-Meier plot results showed that following Ara-C treatment, in comparison with NC control, a prolonged survival was observed in shGILT-injected mice (Fig 5A). Leukemia burden was examined on Day

Table 1
Patient variables and clinical signatures stratified by GILT expression

	Overall population	GILT high	GILT low	P value
Total of patients	87	23	21	
Age, y				0.1
Median	49	51	47	
Range	(16-78)	(21-68)	(26-64)	
WBC $\times 10^9$/L				0.04
Median	18.36	30.29	20.915	
Range	(0.78-308.59)	(5.1-219.1)	(0.78-168.3)	
>50	22	12	3	0.0114
Bone Marrow Blasts (%)				0.0672
Median	62	52	68	
Range	(22-99)	(36-99)	(36-99)	
Risk category				0.0227
Favorable and Intermediate	70	15	20	
Adverse	17	8	1	

WBC, white blood cell count

23 by flow cytometry, and the bone marrows of mice were used to detect cells double positive for human CD45 and GFP. The results showed an inferior percentage of the mice bearing MOLM13 shGILT, indicating that the leukemia burden in these mice was lower than control (Fig 5B). The spleen sizes were also compared, and immunohistochemistry experiments were performed to further characterize AML infiltration. As expected, less spleen enlargement was seen in shGILT AML mice, in comparison with NC mice after Ara-C treatment (Fig 5C). Moreover, less AML cells were detected in the femurs, spleens, and livers of mice injected with MOLM13 shGILT cells as calculated by the mean integrated optical density (IOD) (Fig. 5D and Fig S7A-7C). The mice bearing NC cells showed more severe infiltration. The immunohistochemical studies were consistent with above results, revealing that the leukemia burden was reduced in the mice introduced with MOLM13 shGILT cells after chemotherapy. In addition, the CellROX, MitoSOX and loss of MMP were also evaluated in the leukemia cells extracted from mouse bone marrow on Day 23, and similar results were obtained in this mouse model as the *in vitro* study (Fig 5E-5G). Altogether, these results indicate that the inhibition of GILT in AML cells can ameliorate outcome during chemotherapy of human AML.

GILT is a potential prognostic marker of AML

To characterize the GILT expression in AML patients, we analyzed the frequency and level of *GILT* in 87 AML patient samples by q-PCR. GILT is heterogeneously expressed in AML patients, with higher level detected in leukemias with monocytic features (namely M4 and M5) classified by the French–American–British (FAB) classification systems (Fig 6A). The data from GSE6891 database also confirmed this result (Fig S8A). We also analyzed the association between GILT expression and common genetic alteration of AML. Patients harboring t (8;21) and t (15;17) were found to be low in GILT expression (Fig 6B and Fig S8B). In addition, there was no significant difference of the GILT expression across the different molecular subgroups (Fig S8C). Next, to examine whether GILT expression had a prognostic significance in AML, we detected the GILT level of AML patients at diagnosis. The samples were divided into high and low GILT expression, with transcript expression levels ≥75% (relative expression to GAPDH ≥10.37%) and ≤25% detected percentage (relative expression to GAPDH≤0.91%) defined as high and low GILT expression, respectively. There was no significant association between GILT expression level and age or the percentage of bone marrow blasts at diagnosis. A high GILT level was correlated with a high WBC count (WBC>30 $\times$ 10^9) at diagnosis. Moreover, adverse-risk karyotype was more frequently detected in GILT-high group (Table 1). Also, we found that the AML patients with a relatively high GILT level had a shorter overall survival using TCGA database (Fig 6C). All these results indicated that GILT is a potential prognostic marker of AML.

Discussion

LSCs are thought to be key to chemoresistance and relapse. We compared the protein levels of CD34+ LSC-enriched BMMCs of high and low responders through high-accuracy mass spectrometry. To our knowledge, the present study is the first research using a mass spectrometry-based DIA quantitative proteomic approach to screen the factors in LSCs contributing to the poor prognosis. The chemoresistant AML cells (data from GSE52919) upregulates certain gene expressions and 33 of them were shared with upregulated proteins in low responders. The 33 factors were shown in the heatmap (Fig 1E), some of which have been abundantly studied as increasing research delved deeply into topics of LSC-corresponded chemoresistance. A recently published project illustrated that CD9, a potential biomarker of LSC population, is able to induce chemo-resistant characteristic of LSCs. [47] In addition, previous studies have reported that HMOX1 (HO-1), MTSS1, SLC2A3 (Glut3) and CSF3R (CD114) were important factors expressed in cancer stem cells, and these proteins play critical roles in chemoresistance. [48-51] These studies further confirmed that our screen strategy is credible and reasonable to search for the factors related to LSC chemoresistance. Despite recent interest in this topic, the role of GILT in AML chemoresistance is still not in hand. To further validate that, the GILT level was compared in CD34+ progenitors extracted from 3 individuals who failed to achieve CR taken at the time before and after the first induction chemotherapy, respectively. GILT showed an increasing trend of expression in persisting LSC-enriched CD34+ cells, as compared with preexisting ones. Previous report has shown the association between GILT expression and treatment response of glioblastoma. [52] On top of that, few studies shed light on the involvement of GILT in chemoresistance of tumors. Loss-of-function studies confirmed that AML cells deleted with GILT were more sensitive to chemotherapeutic agents. Here, our work is the first to demonstrate that GILT inhibition attenuate chemoresistance in AML cells both *in vitro and in vivo*.

Oxidative stress has long been linked to cancer initiation and progression, and several reports also demonstrated its association with chemoresistance. [41,53-55] Furthermore, targeting LSC metabolism has become an emerging approach to the development of new chemotherapeutic regimens as the idea concerning that LSCs and bulk leukemia blasts have distinguished metabolic strategy. It has been shown that ROS-low LSCs are more sensitive to BCL-2 inhibitor because they are unable to preserve energy supplies in response to BCL-2 inhibition, with the underlying mechanisms pointing to the impaired oxidative phosphorylation in ROS-low LSCs that lack a compensatory energy production from glycolysis. [15] The LSCs are benefit from the intracellular ROS-low environment in which they can alleviate internal and external stress to support their proliferation. [56] The most common stress the tumor cells encounter was chemotherapy or radiotherapy, and therefore increasing recognition of resistance by ROS-low LSCs comes to attention. One study demonstrated that the prostate CSC has increased survival potential after ionizing radiation due to the ability to recede oxidative stress and to refrain from ROS-induced damage. [57] Another study showed a naturally occurring small molecule named parthenolide (PTL) triggered LSC-specific apoptosis through increasing ROS production to disrupt the redox homeostasis, [39] All the studies indicate that perturbation of ROS-related pathways in LSC may be an effective strategy to eradicate the highly chemo-resistant tumor population. In line with these studies, here, we demonstrated that GILT inhibition could improve treatment response of AML by promoting excessive production of ROS, leading to decreased mitochondrial membrane potential and strengthened Ara-C-induced apoptosis, further providing novel insights that regulation of GILT-mediated redox metabolism might overcome chemoresistance of LSCs.

PI3K/Akt pathway is essential for redox homeostasis, sustaining ROS at a stable level. [45] The excessive ROS is as a result of increased ROS

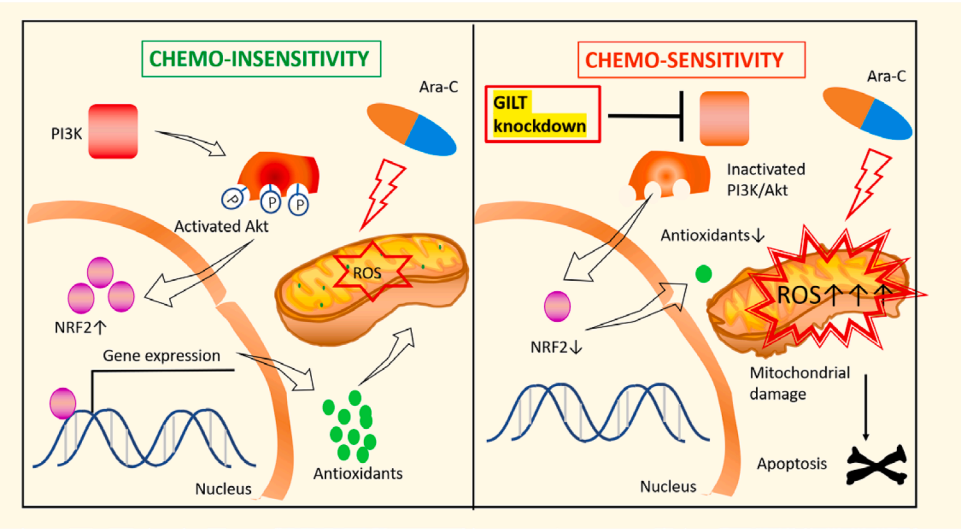

Fig 7. GILT inhibition overcomes chemoresistance in AML
Left panel. Despite that Ara-C stimulates ROS generation and causes oxidative stress, chemoresistance can still develop as a result of compensatory elevation of antioxidants that detoxify the harmful oxidants. Activation of P13K/Akt/NRF2 pathway promotes expression of antioxidants.
Right panel. GILT knockdown facilitates disturbance of redox homeostasis of AML cell by (i) enhancing Ara-C-stimulated ROS overproduction, (ii) reducing antioxidant level which is associated with inactivation of the P13K/Akt/NRF2 axis. The resulting severe oxidative stress leads to mitochondrial damage and apoptosis.

production or declined ROS scavenging systems. NRF2, a transcriptional factor that promotes the expression of several antioxidant enzymes, has been identified as a vital mediator of ROS eradication. [43] There has been much discussion about the role of PI3K/Akt/NRF2 pathway in chemoresistance for its effect on promoting cancer survival by conferring protection against excessive oxidative stress. [58-60] An attractive therapeutic prospect of perturbing redox homeostasis in tumors points to target PI3K/Akt/NRF2 signaling to re-sensitize cancer cells and attenuate chemoresistance. A good example for that is a study by, Liu et al who reported the Diosmetin-induced apoptosis of non-small cell lung cancer (NSCLC) cells in which ROS was accumulated via inhibition of PI3K/Akt/NRF2 pathway. [61] In the present research, our results showed that this axis was repressed in GILT ablation group following Ara-C treatment, promoting an increased understanding of the role of PI3K/Akt/NRF2 pathway in the regulation of ROS-mediated chemoresistance.

GILT may potentially play a pivotal role in regulating the chemoresistance of LSC since GILT is screened from LSCs-enriched CD34+ AML cells, with other factors screened out by our cohorts have been found to be associated with LSC chemoresistance such as CD9. GILT expression was comparable between CD34+ AML blasts and normal CD34+ progenitor cells (data not shown), indicating that GILT is likely a factor of stemness signature, although whether GILT could influence the LSC stemness still needs to be further elucidated. Larger number of samples and deeper studies were needed to more correctly analyze the effects of GILT on the regulation of stemness in both LSC and HSC. Besides, a more detailed analysis between GILT expression and prognosis still needs to be performed in larger clinical cohorts, multi-center studies and longer follow-up. Nevertheless, we have provided new insights into the metabolic regulating role of GILT as a critical mechanism underlying AML chemoresistance.

In summary, GILT is a candidate screened from chemoresisant LSC-enriched CD34+ AML cells. We find that inhibition of GILT can sensitize AML cells to chemotherapy treatment via promoting ROS-mediated mitochondrial damage and apoptosis, at least partially through blockade of the PI3K/Akt/NRF2 pathway (Fig 7). The clinical data have shown that high GILT expression is related to a poor prognosis of AML, suggesting that GILT may be a new target for attenuating chemoresistance in AML.

Conclusion

In summary, GILT is a candidate screened from chemoresisant LSC-enriched CD34+ AML cells. We find that inhibition of GILT can sensitize AML cells to chemotherapy treatment via promoting ROS-mediated mitochondrial damage and apoptosis, at least partially through blockade of the PI3K/Akt/NRF2 pathway. (Fig 7) The clinical data have shown that high GILT expression is related to a poor prognosis of AML, suggesting that GILT may be a new target for attenuating chemoresistance in AML.

Data availability statement

Data that support the findings of this study have been deposited in iProX (integrated proteome resources) Proteomege under the accession code PXD025114. The data that support the findings of this study are available from the corXchanresponding author upon reasonable request.

CRediT authorship contribution statement

Li-Ting Niu: Investigation, Writing – original draft, Visualization, Formal analysis. **Yu-Qing Wang:** Writing – original draft, Validation. **Catherine C.L. Wong:** Investigation, Software. **Shuai-Xin Gao:** Investigation, Data curation. **Xiao-Dong Mo:** Resources. **Xiao-Jun Huang:** Conceptualization, Methodology, Writing – review & editing, Supervision, Project administration, Funding acquisition.

Declaration of Competing Interest

The authors have declared no conflicts of interest.

Acknowledgements

This work was supported by Key Program of the National Natural Science Foundation of China (No.81930004, 81530046), National Key Research and Development Program of China (no. 2017YFA0104500) and Innovative Research Groups of the National Natural Science Foundation of China (no. 81621001)

Supplementary materials

Supplementary material associated with this article can be found, in the online version, at doi:10.1016/j.tranon.2021.101159.

References

[1] H Dohner, DJ Weisdorf, CD. Bloomfield, Acute myeloid leukemia, N. Engl. J. Med. 373 (12) (2015) 1136–1152.

[2] H Guo, YJ Chang, Y Hong, LP Xu, Y Wang, XH Zhang, et al., Dynamic immune profiling identifies the stronger graft-versus-leukemia (GVL) effects with haploidentical allografts compared to HLA-matched stem cell transplantation, Cell Mol. Immunol. (2021).

[3] Y Wang, H Chen, J Chen, M Han, J Hu, H Jiong, et al., The consensus on the monitoring, treatment, and prevention of leukemia relapse after allogeneic hematopoietic stem cell transplantation in China, Cancer Lett. 438 (2018) 63–75.

[4] Y Tan, Q Wu, F. Zhou, Targeting acute myeloid leukemia stem cells: Current therapies in development and potential strategies with new dimensions, Crit. Rev. Oncol. Hematol. 152 (2020), 102993.

[5] D Hanekamp, B Denys, GJL Kaspers, JG Te Marvelde, GJ Schuurhuis, V De Haas, et al., Leukaemic stem cell load at diagnosis predicts the development of relapse in young acute myeloid leukaemia patients, Br. J. Haematol. 183 (3) (2018) 512–516.

[6] JD Hayes, AT Dinkova-Kostova, KD. Tew, Oxidative stress in cancer, Cancer Cell. 38 (2) (2020) 167–197.

[7] E Groninger, GJ Meeuwsen-De Boer, SS De Graaf, WA Kamps, ES. De Bont, Vincristine induced apoptosis in acute lymphoblastic leukaemia cells: a mitochondrial controlled pathway regulated by reactive oxygen species? Int. J. Oncol. 21 (6) (2002) 1339–1345.

[8] H Mizutani, S Tada-Oikawa, Y Hiraku, M Kojima, S. Kawanishi, Mechanism of apoptosis induced by doxorubicin through the generation of hydrogen peroxide, Life Sci. 76 (13) (2005) 1439–1453.

[9] MF Romano, A Lamberti, R Bisogni, P Tassone, D Pagnini, G Storti, et al., Enhancement of cytosine arabinoside-induced apoptosis in human myeloblastic leukemia cells by NF-kappa B/Rel- specific decoy oligodeoxynucleotides, Gene Ther. 7 (14) (2000) 1234–1237.

[10] S Kanno, A Higurashi, Y Watanabe, A Shouji, K Asou, M. Ishikawa, Susceptibility to cytosine arabinoside (Ara-C)-induced cytotoxicity in human leukemia cell lines, Toxicol. Lett. 152 (2) (2004) 149–158.

[11] BC Dickinson, CJ. Chang, Chemistry and biology of reactive oxygen species in signaling or stress responses, Nat. Chem. Biol. 7 (8) (2011) 504–511.

[12] V Helfinger, K. Schröder, Redox control in cancer development and progression, Mol. Aspects Med. 63 (2018) 88–98.

[13] X Shi, Y Zhang, J Zheng, J. Pan, Reactive oxygen species in cancer stem cells, Antioxid. Redox. Signal. 16 (11) (2012) 1215–1228.

[14] DA Pollyea, BM Stevens, CL Jones, A Winters, S Pei, M Minhajuddin, et al., Venetoclax with azacitidine disrupts energy metabolism and targets leukemia stem cells in patients with acute myeloid leukemia, Nat. Med. 24 (12) (2018) 1859–1866.

[15] ED Lagadinou, A Sach, K Callahan, RM Rossi, SJ Neering, M Minhajuddin, et al., BCL-2 inhibition targets oxidative phosphorylation and selectively eradicates quiescent human leukemia stem cells, Cell Stem Cell. 12 (3) (2013) 329–341.

[16] CL Jones, BM Stevens, A D'Alessandro, R Culp-Hill, JA Reisz, S Pei, et al., Cysteine depletion targets leukemia stem cells through inhibition of electron transport complex II, Blood 134 (4) (2019) 389–394.

[17] X Hao, H Gu, C Chen, D Huang, Y Zhao, L Xie, et al., Metabolic imaging reveals a unique preference of symmetric cell division and homing of leukemia-initiating cells in an endosteal niche, Cell Metab. 29 (4) (2019) 950–965. .e6.

[18] MP Rausch, KT. Hastings, Diverse cellular and organismal functions of the lysosomal thiol reductase GILT, Mol. Immunol. 68 (2 Pt A) (2015) 124–128.

[19] B Bogunovic, M Stojakovic, L Chen, M. Maric, An unexpected functional link between lysosomal thiol reductase and mitochondrial manganese superoxide dismutase, J. Biol. Chem. 283 (14) (2008) 8855–8862.

[20] HS Chiang, M. Maric, Lysosomal thiol reductase negatively regulates autophagy by altering glutathione synthesis and oxidation, Free Radic. Biol. Med. 51 (3) (2011) 688–699.

[21] M Maric, I Barjaktarevic, B Bogunovic, M Stojakovic, C Maric, S. Vukmanovic, Cutting edge: developmental up-regulation of IFN-gamma-inducible lysosomal thiol reductase expression leads to reduced T cell sensitivity and less severe autoimmunity, J. Immunol. 182 (2) (2009) 746–750.

[22] AS Advani, B Cooper, V Visconte, P Elson, R Chan, J Carew, et al., A Phase I/II trial of MEC (Mitoxantrone, Etoposide, Cytarabine) in combination with ixazomib for relapsed refractory acute myeloid leukemia, Clin. Cancer Res. 25 (14) (2019) 4231–4237.

[23] D Bonnet, JE. Dick, Human acute myeloid leukemia is organized as a hierarchy that originates from a primitive hematopoietic cell, Nat. Med. 3 (7) (1997) 730–737.

[24] T Lapidot, C Sirard, J Vormoor, B Murdoch, T Hoang, J Caceres-Cortes, et al., A cell initiating human acute myeloid leukaemia after transplantation into SCID mice, Nature 367 (6464) (1994) 645–648.

[25] JK Warner, JC Wang, KJ Hope, L Jin, JE Dick, Concepts of human leukemic development, Oncogene 23 (43) (2004) 7164–7177.

[26] JC Wang, JE. Dick, Cancer stem cells: lessons from leukemia, Trends Cell Biol. 15 (9) (2005) 494–501.

[27] JJ Schuringa, H. Schepers, Ex vivo assays to study self-renewal and long-term expansion of genetically modified primary human acute myeloid leukemia stem cells, Methods Mol. Biol. 538 (2009) 287–300.

[28] D van Gosliga, H Schepers, A Rizo, D van der Kolk, E Vellenga, JJ. Schuringa, Establishing long-term cultures with self-renewing acute myeloid leukemia stem/progenitor cells, Exp. Hematol. 35 (10) (2007) 1538–1549.

[29] Andrews R, Singer J, Bernstein IJTJoem. Human hematopoietic precursors in long-term culture: single CD34+ cells that lack detectable T cell, B cell, and myeloid cell antigens produce multiple colony-forming cells when cultured with marrow stromal cells. 1990;172(1):355-8.

[30] W Tian, N Zhang, R Jin, Y Feng, S Wang, S Gao, et al., Immune suppression in the early stage of COVID-19 disease, Nat. Commun. 11 (1) (2020) 5859.

[31] N Percie du Sert, V Hurst, A Ahluwalia, S Alam, MT Avey, M Baker, et al., The ARRIVE guidelines 2.0: updated guidelines for reporting animal research, PLoS Biol. 18 (7) (2020), e3000410.

[32] HZ Guo, LT Niu, WT Qiang, J Chen, J Wang, H Yang, et al., Leukemic IL-17RB signaling regulates leukemic survival and chemoresistance, FASEB J. 33 (8) (2019) 9565–9576.

[33] SA Bustin, V Benes, JA Garson, J Hellemans, J Huggett, M Kubista, et al., The MIQE guidelines: minimum information for publication of quantitative real-time PCR experiments, Clin. Chem. 55 (4) (2009) 611–622.

[34] T Karantanos, RJ. Jones, Acute myeloid leukemia stem cell heterogeneity and its clinical relevance, Adv. Exp. Med. Biol. 1139 (2019) 153–169.

[35] J Felipe Rico, DC Hassane, ML Guzman, Acute myelogenous leukemia stem cells: from Bench to Bedside, Cancer Lett. 338 (1) (2013) 4–9.

[36] H Wang, D Zhao, LX Nguyen, H Wu, L Li, D Dong, et al., Targeting cell membrane HDM2: A novel therapeutic approach for acute myeloid leukemia, Leukemia 34 (1) (2020) 75–86.

[37] A Abraham, S Varatharajan, S Karathedath, C Philip, KM Lakshmi, AK Jayavelu, et al., RNA expression of genes involved in cytarabine metabolism and transport predicts cytarabine response in acute myeloid leukemia, Pharmacogenomics 16 (8) (2015) 877–890.

[38] S Sriskanthadevan, DV Jeyaraju, TE Chung, S Prabha, W Xu, M Skrtic, et al., AML cells have low spare reserve capacity in their respiratory chain that renders them susceptible to oxidative metabolic stress, Blood 125 (13) (2015) 2120–2130.

[39] ML Guzman, RM Rossi, L Karnischky, X Li, DR Peterson, DS Howard, CT. Jordan, The sesquiterpene lactone parthenolide induces apoptosis of human acute myelogenous leukemia stem and progenitor cells, Blood 105 (11) (2005) 4163–4169.

[40] S Pei, M Minhajuddin, KP Callahan, M Balys, JM Ashton, SJ Neering, et al., Targeting aberrant glutathione metabolism to eradicate human acute myelogenous leukemia cells, J. Biol. Chem. 288 (47) (2013) 33542–33558.

[41] Y Chen, Y Liang, X Luo, Q. Hu, Oxidative resistance of leukemic stem cells and oxidative damage to hematopoietic stem cells under pro-oxidative therapy, Cell Death. Dis. 11 (4) (2020) 291.

[42] EK Kim, M Jang, MJ Song, D Kim, Y Kim, HH. Jang, Redox-mediated mechanism of chemoresistance in cancer cells, Antioxidants (Basel) 8 (10) (2019).

[43] D Xue, X Zhou, J. Qiu, Emerging role of NRF2 in ROS-mediated tumor chemoresistance, Biomed. Pharmacother. 131 (2020), 110676.

[44] ER Macari, EK Schaeffer, RJ West, CH. Lowrey, Simvastatin and t-butylhydroquinone suppress KLF1 and BCL11A gene expression and additively increase fetal hemoglobin in primary human erythroid cells, Blood 121 (5) (2013) 830–839.

[45] N Koundouros, G. Poulogiannis, Phosphoinositide 3-Kinase/Akt signaling and redox metabolism in cancer, Front. Oncol. 8 (2018) 160.

[46] Y Yang, B Liu, J Xu, J Wang, J Wu, C Shi, et al., Derivation of pluripotent stem cells with in vivo embryonic and extraembryonic potency, Cell 169 (2) (2017) 243–257. .e25.

[47] Y Liu, G Wang, J Zhang, X Chen, H Xu, G Heng, et al., CD9, a potential leukemia stem cell marker, regulates drug resistance and leukemia development in acute myeloid leukemia, Stem Cell Res. Ther. 12 (1) (2021) 86.

[48] N Zhe, J Wang, S Chen, X Lin, Q Chai, Y Zhang, et al., Heme oxygenase-1 plays a crucial role in chemoresistance in acute myeloid leukemia, Hematology 20 (7) (2015) 384–391.

[49] M Schemionek, O Herrmann, MM Reher, N Chatain, C Schubert, IG Costa, et al., Mtss1 is a critical epigenetically regulated tumor suppressor in CML, Leukemia 30 (4) (2016) 823–832.

[50] É Cosset, S Ilmjärv, V Dutoit, K Elliott, T von Schalscha, MF Camargo, et al., Glut3 addiction is a druggable vulnerability for a molecularly defined subpopulation of glioblastoma, Cancer Cell 32 (6) (2017) 856–868. .e5.

[51] PE Zage, SB Whittle, JM. Shohet, CD114: a new member of the neural crest-derived cancer stem cell marker family, J. Cell. Biochem. 118 (2) (2017) 221–231.

[52] C Zhu, X Chen, G Guan, C Zou, Q Guo, P Cheng, et al., IFI30 is a novel immune-related target with predicting value of prognosis and treatment response in glioblastoma, Onco Targets Ther. 13 (2020) 1129–1143.

[53] PM Bruno, Y Liu, GY Park, J Murai, CE Koch, TJ Eisen, et al., A subset of platinum-containing chemotherapeutic agents kills cells by inducing ribosome biogenesis stress, Nat. Med. 23 (4) (2017) 461–471.

[54] L Shi, L Wu, Z Chen, J Yang, X Chen, F Yu, et al., MiR-141 activates Nrf2-dependent antioxidant pathway via down-regulating the expression of Keap1 conferring the resistance of hepatocellular carcinoma cells to 5-fluorouracil, Cell. Physiol. Biochem. 35 (6) (2015) 2333–2348.

[55] S Nobrega-Pereira, F Caiado, T Carvalho, I Matias, G Graca, LG Goncalves, et al., VEGFR2-mediated reprogramming of mitochondrial metabolism regulates the sensitivity of acute myeloid leukemia to chemotherapy, Cancer Res. 78 (3) (2018) 731–741.

[56] D Zhou, L Shao, DR. Spitz, Reactive oxygen species in normal and tumor stem cells, Adv. Cancer. Res. 122 (2014) 1–67.

[57] YS Kim, MJ Kang, YM. Cho, Low production of reactive oxygen species and high DNA repair: mechanism of radioresistance of prostate cancer stem cells, Anticancer Res. 33 (10) (2013) 4469–4474.

[58] L Qiu, Z Ma, X Li, Y Deng, G Duan, LE Zhao, et al., DJ-1 is involved in the multidrug resistance of SGC7901 gastric cancer cells through PTEN/PI3K/Akt/Nrf2 pathway, Acta Biochim. Biophys. Sin. (Shanghai) 52 (11) (2020) 1202–1214.

[59] Y Li, Y Guo, Z Feng, R Bergan, B Li, Y Qin, et al., Involvement of the PI3K/Akt/Nrf2 signaling pathway in resveratrol-mediated reversal of drug resistance in HL-60/ADR cells, Nutr. Cancer 71 (6) (2019) 1007–1018.
[60] J Yao, X Wei, Y. Lu, Chaetominine reduces MRP1-mediated drug resistance via inhibiting PI3K/Akt/Nrf2 signaling pathway in K562/Adr human leukemia cells, Biochem. Biophys. Res. Commun. 473 (4) (2016) 867–873.
[61] X Chen, Q Wu, Y Chen, J Zhang, H Li, Z Yang, et al., Diosmetin induces apoptosis and enhances the chemotherapeutic efficacy of paclitaxel in non-small cell lung cancer cells via Nrf2 inhibition, Br. J. Pharmacol. 176 (12) (2019) 2079–2094.